Determination of the Rydberg Constant from the Emission Spectra of H and He+

Kyle D. Shaffer
Department of Chemistry, West Chester University of Pennsylvania, ks898423@wcupa.edu

Recommended Citation

Introduction

The absorption or emission of a photon or another form of energy may cause a transition between electronic energy levels in a given atom. When a photon is absorbed, all of its energy is transferred to the atom. In order for a transition between states to occur, the energy of the photon absorbed must be equivalent to the energy difference between these states. Once this transition occurs and the electron has been promoted to a higher energy state, it will spontaneously relax back to its original ground state and may release another photon by fluorescence. The energy levels of a hydrogen atom can be described by the Bohr model of the atom. Other atoms can be simplified to fit this structure as well if they are in the form of hydrogenic ions, meaning they contain only one electron. The wavenumber in cm^{-1} of the lines in the spectra of hydrogen and hydrogenic ions can be represented by the *Rydberg formula*:

$$(1) \qquad \tilde{v} = \frac{1}{\lambda} = Z^2 R_X \left(\frac{1}{n_1^2} - \frac{1}{n_2^2} \right)$$

where λ is the wavelength of the emitted photon in cm, Z is the nuclear charge of the atom, n_1 is the principal quantum number of the state returned to after radiative relaxation, n_2 is the quantum number of the initial state before radiative relaxation, and R_X is the Rydberg constant for the hydrogenic ion or H atom being analyzed. R_X has the identity of:

$$(2) \qquad R_X = \frac{\mu e^4}{8 \varepsilon_0^2 h^3 c}$$

where e is the elementary charge (1.60217649 x 10^{-19} C), ε_0 is the vacuum permittivity constant (8.85418782 x 10^{-12} C^2 J^{-1} m^{-1}), h is Planck's constant (6.62606896 x 10^{-34} J s) and c is the speed of light in vacuum (2.99792458 x 10^8 m s^{-1}) [1]. Each hydrogenic atom has its own unique value of R_X due to slight shifts in reduced mass μ, defined by:

$$(3) \qquad \mu = \frac{m_e m_{nucleus}}{m_e + m_{nucleus}}$$

in kg [1]. These values of R_X converge on a value for the Rydberg constant with an infinitely massive nucleus R_∞, 109 737.31568076 cm^{-1} [2]. Theoretical calculation of this constant leads to extreme accuracy given the simplicity of the H atom, to the 12th decimal place. High-resolution laser spectroscopy leads to even more accurate measurement, up to the 15th decimal place from the study of the 1S to 2S transition, making it the most precise transition frequency calculated for H thus far and making the Rydberg constant R_∞ the most accurately measured fundamental physical constant [3]. This value is not the constant for the hydrogen atom, however, since it uses an infinite mass. When the reduced mass of a hydrogen atom is substituted

into Equation 2, the Rydberg constant for hydrogen R_H is determined to have a value of 109 677.581 cm^{-1} [1]. Using a ratio between the reduced masses of H and He$^+$, a value for R_{He} can be calculated fairly effortlessly. Using both the values of R_X determined for H and He$^+$ and substituting them into Equation 1 with valid quantum numbers for state transitions, a simulated line spectrum can be constructed to estimate the wavenumbers and wavelengths in which transitions occur. This technique can be applied to any hydrogenic atom.

The proton is one of the fundamental building blocks of the universe and its study has led the development of modern physics and chemistry. By using high-resolution laser spectroscopy techniques involving hydrogen and its derivatives, such as deuterium and muonic hydrogen (a proton being orbited by a negatively charged muon instead of an electron), new properties of atoms are being discovered or iterated to find an accurate model of the system. Two of such properties are the anomalous, magnetic moment of hydrogen and the proton charge radius r_p. The proton charge radius is the root-mean-square of its charge distribution. In other words, it is the measure of the size of the atomic nucleus, which in a hydrogen atom, is just the size of a proton. The most accurate description of r_p, with an uncertainty of 1 percent, is given by the compilation of constants by the Committee on Data for Science and Technology (CODATA) with a value of 0.8414 fm. This value was determined from 24 precision spectroscopic measurements of the transition frequencies of hydrogen and deuterium and elastic electron scattering [4]. That being said, the accuracy of this value for r_p, determined by hydrogen independent electron-proton scattering, limits the quantification of the Rydberg constant as well as testing of bound-state quantum electrodynamics (QED). An attractive area of study to increase the accuracy of this value is in the measurement of r_p using muonic hydrogen. Spectroscopic data analysis has determined there is a four to five standard deviation discrepancy between the charge radius of normal hydrogen and the charge radius of the exotic muonic hydrogen. This is due to the muon's orbit being 200 times smaller than the orbit of the electron around the proton nucleus. This results in a seven order of magnitude increase of the influence of the charge radius on the electronic energy levels of the orbiting particle [3].

In 2010, Pohl *et al.* conducted a study using pulsed laser spectroscopy to measure the Lamb shift of muonic hydrogen. Calculating the frequency of the Lamb shift, the energy spacing between the $2S_{1/2}$ and the $2P_{1/2}$ states not predicted by the Dirac equation, resulted in as much as a 2 percent change in the expected transition frequency from hydrogen. Through subsequent calculation using the fine and hyperfine splitting of spectral lines and QED terms, the group found the value of r_p to be 0.84184(67) fm, a whole 5 standard deviations lower than the accepted value at the time of 0.8768(69) fm from CODATA (the numbers in parenthesis indicate the 1 standard deviation uncertainty of the trailing digits of the given number). This

new value was used in accordance with the most recent value at the time, the fine structure constant α, to calculate the Rydberg constant. Based off of this acquired data and extrapolation to transitions such as 1S to 2S, two conclusions were proposed: either the Rydberg constant needed to be shifted by -110 kHz c^{-1} (-3.669 x 10^{-6} cm^{-1}) or the calculations of the quantum electrodynamic effects of hydrogen and muonic hydrogen are insufficient [3].

In a more recent study published in 2017 by Beyer *et al.*, a similar experiment was conducted. In this case, the transition frequency of the 2S to 4P transition was studied to determine the charge radius and the effects of quantum interference on the discrepancy of the calculation. In this study, though, the four standard deviation discrepancy between the charge radius determined of normal H and muonic hydrogen was investigated and tested using a cryogenic beam of H atoms. A 243 nm laser was used to promote H atoms being propelled through a cold copper nozzle at 5.8 K from the ground state (1S) to the 2S state. This was performed by a two-photon excitation system of two phase-retracing antiparallel laser beams in order to induce Doppler shifts of equal magnitude but opposite signs upon the atoms being transitioned to the 2S state. This beam of almost exclusively 2S H atoms was then crossed perpendicularly to a spectroscopy laser at 486 nm to induce the two possible 2S to 4P dipole allowed transitions (4P$_{1/2}$ or 4P$_{3/2}$). In order to observe the effects of quantum interference, the large, solid-angle detector was split by a vertical wall in line with the spectroscopy laser beam, forcing two detectors observing the fluorescence from the 4P state at the same solid angle but from different directions. The short-lived 4P state decayed rapidly back to the ground state, emitting a Lyman-γ extreme ultraviolet photon, which stimulated the release of a photoelectron from the graphite coated inner walls of the detector. These photoelectrons were then counted by one of the two channel electron multipliers, giving a readable signal [6].

Quantum interference typically causes distortions in line shape from the superpositions of the emitted photons crossing their own trajectory and affecting the direction of their paths, or by many resonances being detected at various geometric laser polarization orientations. In this experiment, the quantum interference was remedied by instituting a Fano-Voigt line shape. The geometry dependence on line shape is removed by the asymmetry parameter of the Voigt approximation ($\eta = 0$). With the geometry dependence gone, the unperturbed transition frequencies can be calculated by averaging over the various laser polarization settings and signals from both detectors. With the transition frequency calculated, in combination with the well-known 1S to 2S transition frequency, the Rydberg constant R$_\infty$ and the proton charge radius r$_p$ were calculated and found to be 109 737.31568076(96) cm^{-1} and 0.8335(95) fm respectively. Both of these values are in agreement with values concluded for the muonic hydrogen analysis

but represent a 3.3 times standard deviation discrepancy from the world data [5]. The conclusion of this experiment is the discrepancies between these data and the world data limit the precision of bound state QED tests and given the QED calculations are correct, the only way to understand the discrepancy is through improved accuracy with new experiments [6]. The fact that the values found were in correlation with the values determined for the muonic hydrogen shows the understanding of particle and laser physics is ever evolving to develop a much better idea of the world on a sub-atomic scale. The determination of the Rydberg constant is the keystone of the accuracy of these measurements.

Experimental

This experiment used several components: a Hydrogen atomic lamp or a Helium atomic lamp attached to the input slit of a 0.5 m grating spectrometer, and a photomultiplier detector (PMT) attached to the output slit. The PMT was also hooked up to a computer with the SciSpec program downloaded onto it for analysis. Before any data were acquired, predictions on peak values were made. To do this, the respective Z values and values for the Rydberg constant for H and He$^+$ must be determined and plugged into Equation 1 in an iterative process performed with varying principal quantum numbers n_1 and n_2 with n_1 held constant per iteration to represent the radiative transition. The PMT can detect wavelengths of light in the visible to UV range (190 nm to 380 nm for UV, 380 nm to 750 nm for visible), so this process determines which combination of n_1 with changing n_2 yields transitions emitting in that range. As the principal quantum number n_2 increases, the wavenumber $\tilde{\nu}$ in cm^{-1} increases but the spacings between the energy levels will decrease, so the values will converge on the lower energy limit of the unbound continuum states. These wavenumber values are then converted to wavelength in order to predict where transition peaks will lie. Simulated line spectra were created for both species in wavenumber and wavelength. The simulated spectra for both species with set n_1 values are shown in Figure 1 below.

(a)
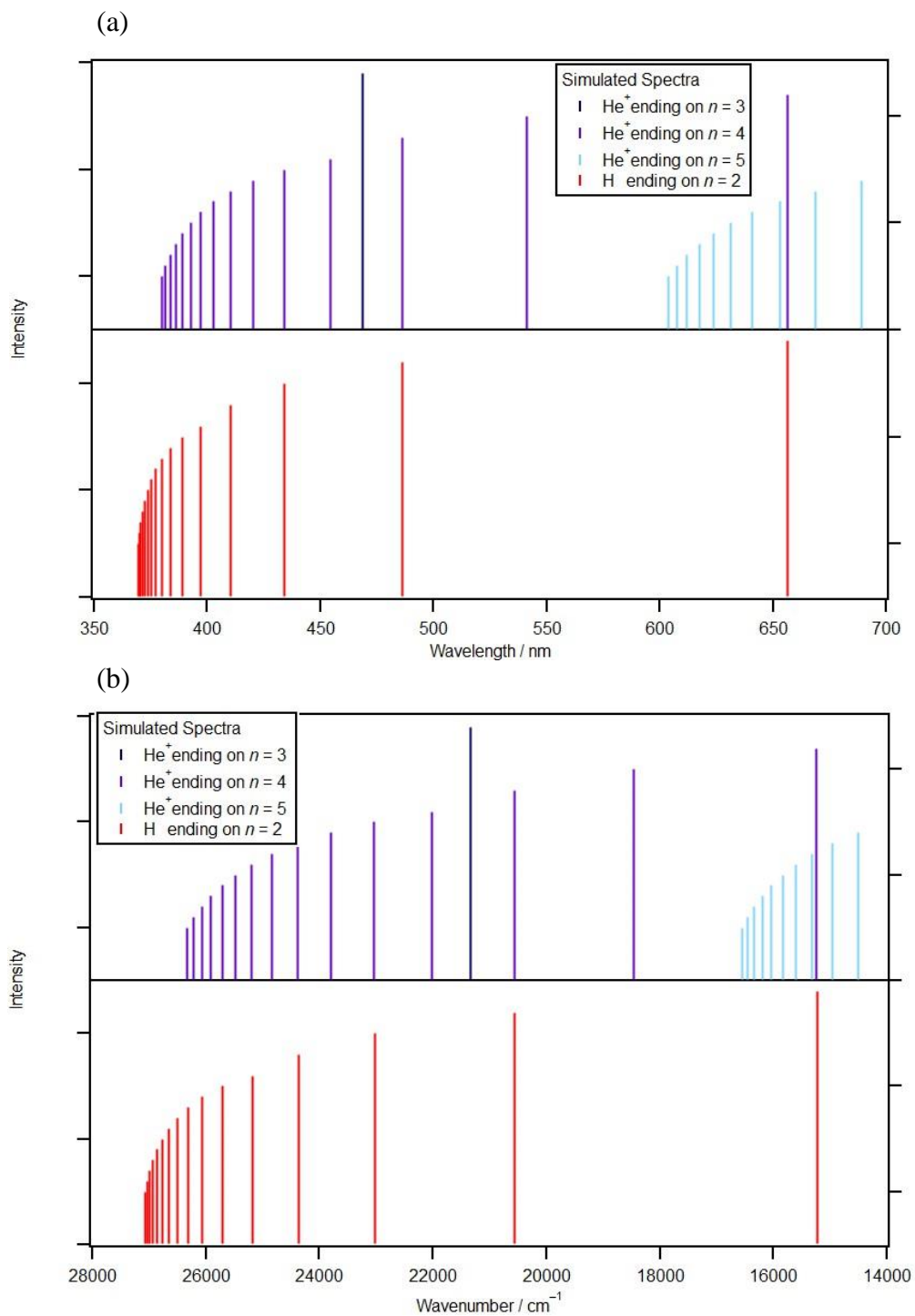

(b)

Figure 1. Simulated emission line spectra for H and He$^+$ with designated transition resting state principal quantum number n_1. (a) simulated peaks in units of wavelength (nm) (b) simulated peaks in units of wavenumber (cm^{-1})

Note in Figure 1 above, the line spectra for transitions to $n_1 = 3$ and 5 are also shown for He^+. This is to demonstrate the iterative process used to determine the transitions found in the UV to visible range of the spectrum. As observed, the $n_1 = 4$ transition makes up the majority of the estimated scanned region. The $n_1 = 3$ transition was not used because it was found to converge in the short-wave UV range, higher in energy than the range being analyzed. The $n_1 = 5$ transition was not used for analysis either. While this transition does converge in the visible range, the first six transitions were found to have emission wavelength values in the infrared region, lower in energy than the region being analyzed. Tables 1 and 2 show the wavenumber and wavelength values for the first 10 transitions of He^+ with an $n_1 = 3$ and 5 respectively. Tables 3 and 4 represent the tabulated predictions of peak positions in the UV to visible region analyzed for the H and He II spectrum respectively.

Table 1. Transition peak values estimated for the He II spectrum with an $n_1 = 3$

Wavenumber / cm^{-1}	Wavelength / nm	Respective Transition
21334.76	468.719	n = 3-4
31209.71	320.413	n = 3-5
36573.88	273.419	n = 3-6
39808.3	251.204	n = 3-7
41907.57	238.620	n = 3-8
43346.82	230.697	n = 3-9
44376.31	225.345	n = 3-10
45138.01	221.543	n = 3-11
45717.35	218.735	n = 3-12
46168.21	216.599	n = 3-13

Table 2. Transition peak values estimated for the He II spectrum with an $n_1 = 5$

Wavenumber / cm^{-1}	Wavelength / nm	Respective Transition
5364.17	1864.221	n = 5-6
8598.59	1162.981	n = 5-7
10697.86	934.766	n = 5-8
12137.11	823.919	n = 5-9
13166.6	759.498	n = 5-10
13928.3	717.963	n = 5-11
14507.64	689.292	n = 5-12
14958.5	668.516	n = 5-13
15316.24	652.902	n = 5-14
15604.85	640.826	n = 5-15

Table 3. Predicted peak values/transition energies for the H spectrum

Wavenumber / cm^{-1}	Wavelength / nm	Respective Transition
15232.997	656.470	n = 2-3
20564.546	486.274	n = 2-4
23032.292	434.173	n = 2-5
24372.796	410.294	n = 2-6
25181.077	397.124	n = 2-7
25705.683	389.019	n = 2-8
26065.351	383.651	n = 2-9
26322.619	379.901	n = 2-10

Table 4. Predicted peak values/transition energies for the He II Spectrum

Wavenumber / cm^{-1}	Wavelength / nm	Respective Transition
9874.94	1012.6644	n = 4-5
15239.12	656.20604	n = 4-6
18473.54	541.31477	n = 4-7
20572.81	486.07847	n = 4-8
22012.06	454.29642	n = 4-9
23041.54	433.99877	n = 4-10
23803.25	420.1107	n = 4-11
24382.59	410.1287	n = 4-12
24833.45	402.68267	n = 4-13
25191.19	396.96418	n = 4-14
25479.8	392.46776	n = 4-15
25716.01	388.86281	n = 4-16
25911.77	385.92501	n = 4-17
26075.82	383.49705	n = 4-18

The true acquired spectra are found in the Results and Discussion section below. Analysis of these peaks showed the specific regions to target for accurate measurements of transition wavelengths in close up scans. Once the predictions were done, data acquisition could begin. The experimental setup is represented in Figure 2 below. As mentioned previously, this experiment utilized two lamps, hydrogen and helium, a 0.5 m diffraction spectrometer, and a photomultiplier detector hooked up to a computer for wavelength analysis. The PMT has the ability to operate at any voltage from 1 - 1000 V, based upon the desired magnitude of signal. It is important to adjust the high voltage (HV) of the PMT so as not to saturate the lower energy signals, since they will be detected first. Saturation of the peaks may distort the peak center by flattening the top of the curve. In order to calibrate this, the lowest energy peak of each spectrum (the highest wavelength) must be focused on and tuned so its signal voltage is between 5 V and 10 V. All

other desired acquired peaks will be below this value. This signal may be adjusted once the readings are well into the blue range and very small.
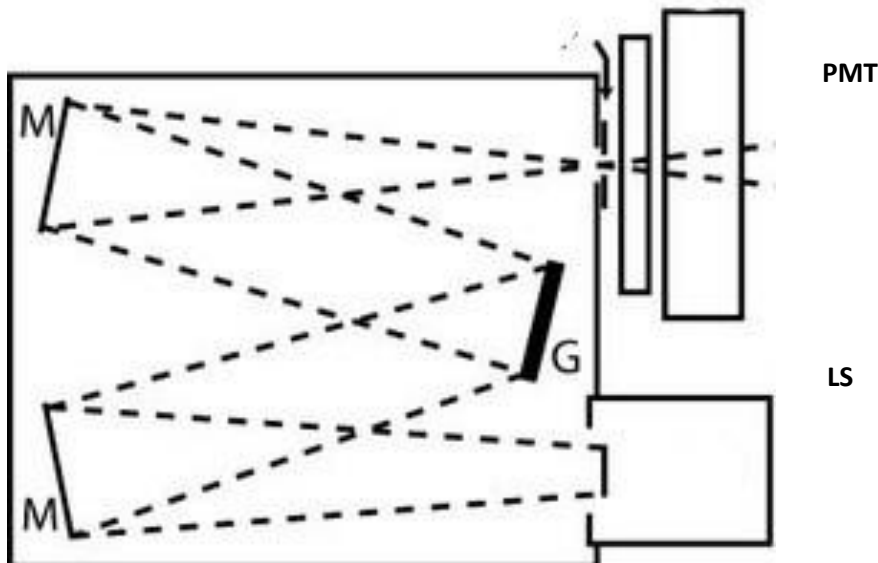

Figure 2. Experimental setup. LS represents the lamp light source, M represent two focusing mirrors present in the grating spectrometer, G is representative of the adjustable diffraction grating that separates the various wavelengths of light, and PMT is the photomultiplier detector positioned at the exit slit.

Another note: as the setting for the HV increases, it will become more sensitive, meaning undesired excess noise will be acquired as well. This may be remedied by adjustment of the exit slit to decrease or increase the light hitting the detector. The hydrogen or helium lamp was then turned on, as well as all other required instrumentation; the PMT was set to 914 V and signal optimization was performed. Once the optimal signal to noise ratio was determined, readings were then taken.

The first set of data taken were broad scans of the full spectrum in nine 30 nm increments. These are inaccurate survey scans used to visualize the full spectrum and where individual peaks desired may be found, roughly. For hydrogen, range of the spectrum was taken from 380 nm to 660 nm and for helium, data were taken from 370 nm to 670 nm. Once the broad survey scans were acquired and predicted peaks were marked, individual peaks were scanned with high resolution. This was done by scanning the region where the peak was expected to be found plus or minus 1 nm. In the low ranges (370 nm to 400 nm), the HV of the PMT was increased to 1000 V and the high-resolution settings were used in place of a survey scan. This is because many peaks are in these regions that are set close together and

with decreasing intensity; therefore, a survey scan would most likely not have a suitable signal-to-noise ratio for analysis of these peaks. After each set of peaks and survey scans was acquired, they were saved as .dat files for editing and calculation in a data analysis software such as Igor Pro 8 [7].

Results and Discussion

After several iterations of calculations, the value for n_1 and n_2, the principal quantum number that yielded transition energies in the UV to visible region, were found to be $n_1 = 2$ for hydrogen and $n_1 = 4$ for helium. Spectra were obtained using the method described and the wavelength values were converted to wavenumber in cm^{-1} by multiplying the respective value by 10^{-7} and then taking the inverse. The data were then compiled onto survey spectra, with the values for hydrogen shown in Figure 3 with a range of 400 nm to 660 nm, and the He II spectrum shown in Figure 4 with a range of 380 nm to 680 nm. Unfortunately, no survey scan data were acquired for the 380 nm to 400 nm region for the hydrogen spectrum, which is where the latter half of the transitions occurred, so those data are not shown in a survey scan format. However, the specific peaks in that region were used in high resolution scans, so they were able to be used for calculation of the Rydberg constant. The helium spectrum shows no clear decreasing trend in its respective spectrum, so therefore principal quantum number transition values were unable to be assigned.
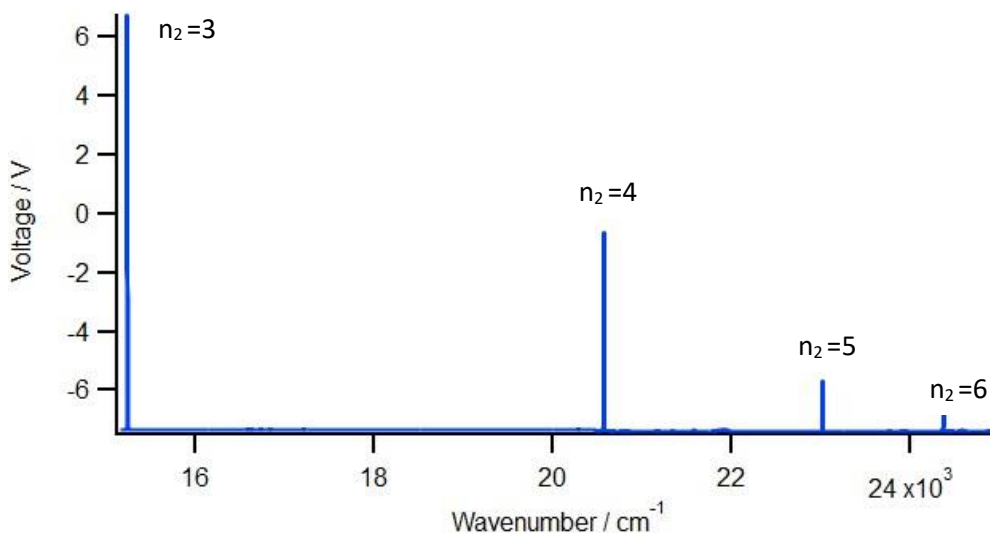

Figure 3. Hydrogen photon emission spectrum with range of 660 nm to 400 nm. Each peak is labelled with its corresponding excited state principal quantum number, n_2.
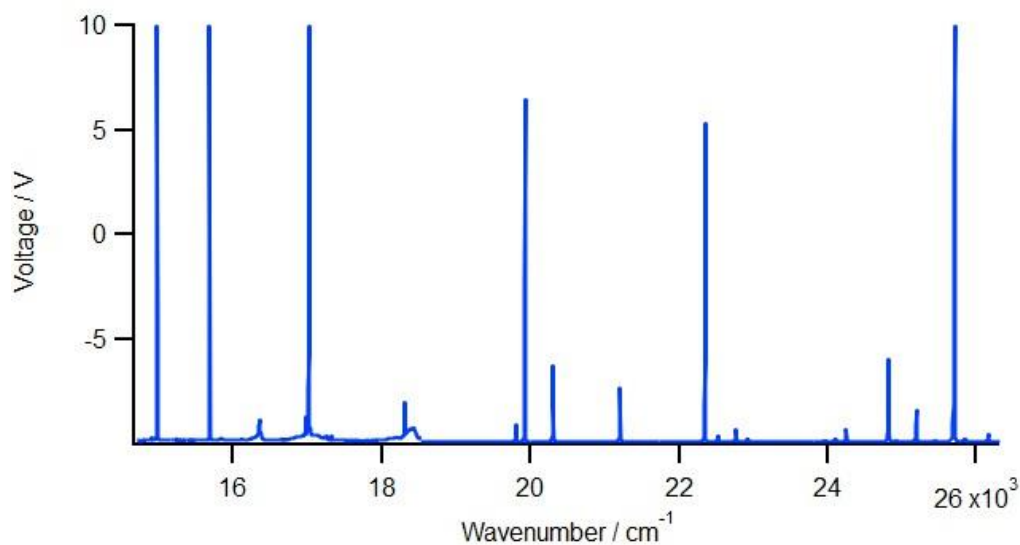
Figure 4. He II photon emission spectrum with a range from 380 nm to 680 nm. The lack of clear trend limited the ability to assign peaks to specific transition quantum numbers.

As can be seen by Figure 4, the He spectrum acquired was quite busy and not as precise as seen in Figure 3 for hydrogen. This is because the helium lamp contains elemental helium, He, which has two electrons and two protons. This is not a hydrogenic atom and therefore has many electronic transitions that cannot be accounted for with a simple Rydberg-like formula because of the increased number of electrostatic interactions and spin-orbit coupling within it. The He^+ ion only accounts for a small amount of the atoms in this system and therefore the signals given off by its electronic transitions are fairly small or superimposed onto other transitions' peaks occurring at similar wavelengths. Another unfortunate occurrence that happened while acquiring data was the data for the high-resolution peaks of the He II spectrum were taken at wavelength values expected for H, not for He^+. This was troublesome until the segments of the scan data proved to contain peaks at the expected wavelengths for the He^+ transitions. The subsequent calculations were made using the peak data from the survey scans of the He II spectrum, contributing to extra error.

Once the full survey scans were plotted, each individual major peak was analyzed by fitting a Lorentzian function to it in order to obtain its true center and the wavenumber associated with that transition. An example of this fitting to the initial transition ($n = 2$ to 3) of the H spectrum is found in Figure 5 below. The tabulated acquired data for each significant peak in the H and He II spectra are found in Tables 5 and 6 respectively.
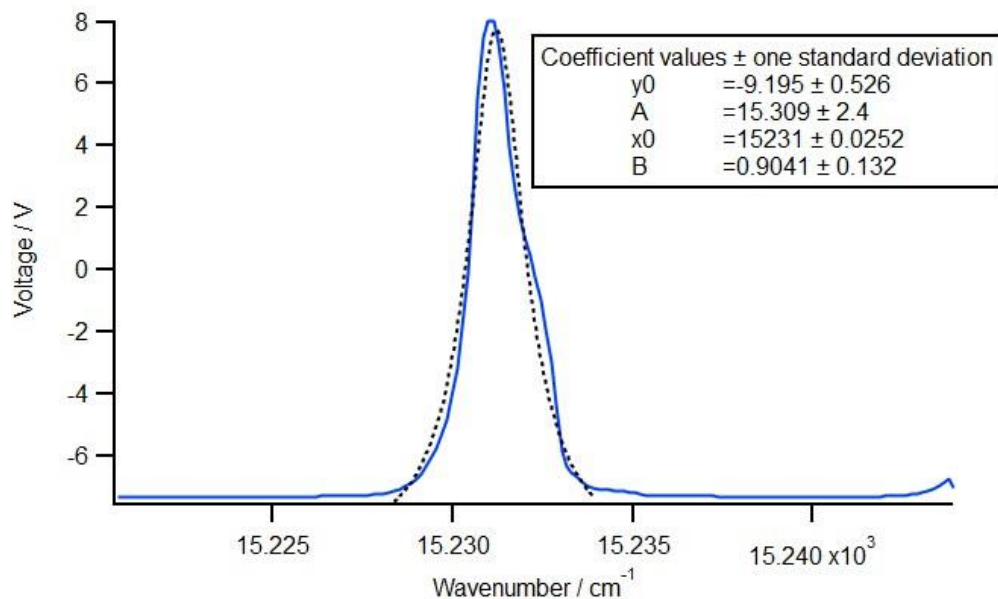
Coefficient values ± one standard deviation
y0   =-9.195 ± 0.526
A   =15.309 ± 2.4
x0   =15231 ± 0.0252
B   =0.9041 ± 0.132

Figure 5. Example of a Lorentzian fitting to the peak center of the $n = 2$ to 3 transition in H. The Lorentzian fit is represented by the dashed line. This particular peak has its center at 15231 cm^{-1}.

Table 5. Tabulated data for major peak locations for the H spectrum and their respective exited state principal quantum numbers n_2.

Wavenumber / cm^{-1}	Wavelength / nm	Excited State Principal Quantum Number (n_2)
15231	656.556	3
20566	486.239	4
23015	434.499	5
24370	410.341	6
25161	397.440	7
25709	388.969	8
26062	383.700	9
26308	380.113	10

Table 6. Tabulated data for major peak locations for the He II spectrum and their respective exited state principal quantum numbers n_2.

Wavenumber / cm^{-1}	Wavelength / nm	Excited State Principal Quantum Number (n_2)
15231	656.5557088	6
18309	546.1794746	7
20302	492.5623091	8
22355	447.3272199	9
22918	436.3382494	10
23958	417.3971116	11
24247	412.4221553	12
24819	402.9171199	13
25192	396.9514131	14
25445	393.0045196	15
25707	388.9991053	16
25848	386.8771278	17
26160	382.2629969	18

Note the $n = 4$ to 5 transition is not present. This is because it had an estimated transition wavelength of 1012.664 nm, which is found in the infrared region of the electromagnetic spectrum, and was not measured.

By manipulation of Equation 1, a linear relation can be found for each H and He$^+$. That manipulation is shown for H as:

(4)
$$\tilde{v} = \frac{R_H}{n_1^2} - \frac{R_H}{n_2^2} = a + bx$$

where the slope is equal to the negative of R$_H$ and the intercept is equal to $\frac{R_H}{n_1^2}$. For He, the manipulation is slightly different since the nuclear charge Z must be taken into account. The resulting linear relation becomes:

(5)
$$\tilde{v} = \frac{4R_{He}}{n_1^2} - \frac{4R_{He}}{n_2^2} = a + bx$$

where the slope is equal to the negative of 4 times R$_{He}$ and the intercept is equal to $\frac{4R_{He}}{n_1^2}$. Each of these equations have a y-value of the wavenumber of the transition and an x-value of n^{-2}. Therefore, since those values are known for each transition as determined by analysis of the spectra, a plot of these values versus each other yielded regression equations that were manipulatable to determine the Rydberg constant for H and He$^+$. When this was performed two linear regression plots were obtained, one for each atom, shown in Figures 6 and 7. The coefficient values are reported with their respective error at the 95% confidence value.
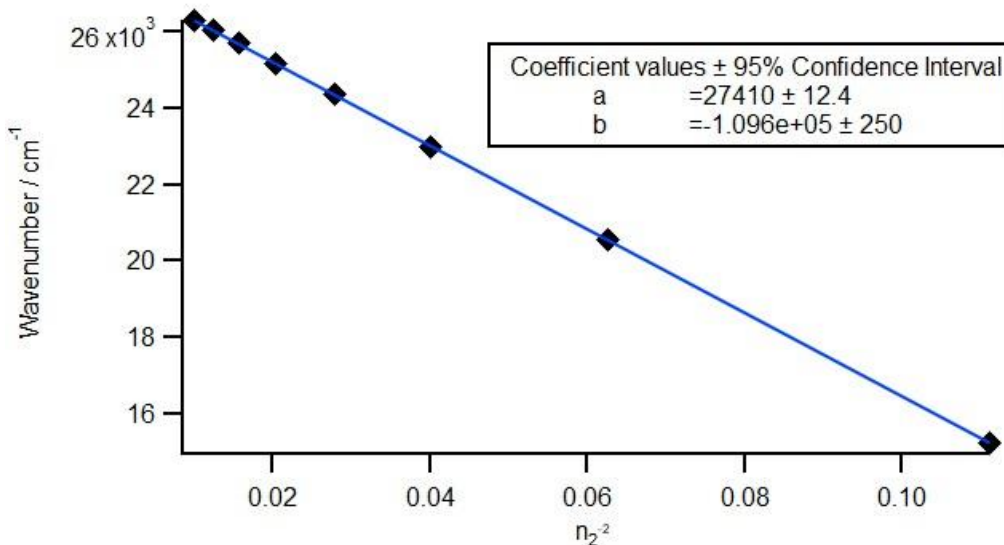
Figure 6. Linear plot relation of the Rydberg formula used to determine the Rydberg constant for H. Associated error at the 95% confidence interval is reported with coefficient values.
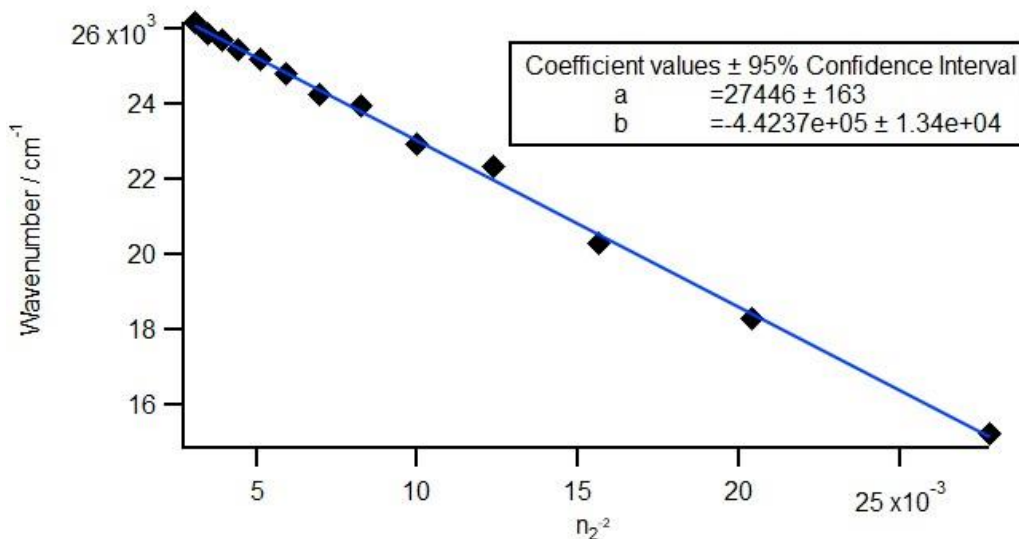

Figure 7. Linear plot relation of the Rydberg formula used to determine the Rydberg constant for He$^+$. Associated error at the 95% confidence interval is reported with coefficient values.

The first manipulation of the slope equations acquired was to confirm the value of n_1. This was performed by dividing the slope by the y-intercept which gives a value for n_1^2. This value was then square rooted to obtain the identity of n_1, which for H was confirmed to be 2 and for He$^+$ was determined to be 4. Using the relationships described above and in Equations 4 and 5, the Rydberg constant for each hydrogen

and He$^+$ were calculated in two ways. For hydrogen, solving the slope relationship yielded an R$_H$ of 109 601.885 cm^{-1}, and solving the intercept relation yielded an R$_H$ of 109 638.554 cm^{-1}. For helium, the slope relation yielded an R$_{He}$ of 110 592.324 cm^{-1} and the intercept relation yielded an R$_{He}$ of 109 783.591cm^{-1} which is incredibly close to the estimated value of R$_{He}$ of 109 721.636 cm^{-1} with a differentiation of only a few wavenumbers.

Error Analysis

The 95% confidence interval of the slope and intercept of each plot was calculated using the linear fit tool in Igor Pro 8 and the interval was reported with the coefficient values shown in Figure 6 and 7. Since the first method of calculation of the Rydberg constant was by use of the slope, the error in that value may be calculated by solving the same relationship. For hydrogen, the error in the slope is equal to the error in the Rydberg constant. This error value was determined to be equal to 250 cm^{-1} (or about 300 cm^{-1} with significant figures). For He$^+$, the error in the slope is 4 times the error in the Rydberg constant, therefore by solving for δR$_{He}$, a value of 3350 cm^{-1} was obtained (or about 3000 cm^{-1} with significant figures).

The error in the intercept for R$_H$ and R$_{He}$ were 12.4 and 163 respectively. To find the corresponding error for the Rydberg constant calculated from that relation, the following equations were used:

(6) $$\delta R_H = \delta intercept * n_1^2 = 12.4 * 4 = 49.6 \; cm^{-1}$$

(7) $$\delta R_{He} = \frac{\delta intercept * n_1^2}{4} = \frac{163 * 16}{4} = 652 \; cm^{-1}$$

Therefore, the error at the 95% confidence interval for R$_H$ and R$_{He}$ when calculated using the intercept were determined to be about 50 cm^{-1} and 700 cm^{-1} respectively, when accounting for significant figures.

Conclusions

The value of the Rydberg constant for the H and He II spectrum was calculated in two ways: by analysis of the slope and intercept of the linear plot of Equation 1. For H, R$_H$ was determined to be 109 600 ± 300 cm^{-1} from analysis of the slope and 109 640 ± 50 cm^{-1} from the intercept with an n_1 value of 2. For He$^+$, R$_{He}$ was determined to be 111 000 ± 3000 cm^{-1} from the slope and 109 800 ± 700 cm^{-1} from the intercept with an n_1 value of 4. The literature value for R$_\infty$, the Rydberg constant of infinite nuclear mass, is 109 737.316 cm^{-1} [2] and the literature value for R$_H$ is 109 677.581 cm^{-1} [1]. For He$^+$ initial calculations estimated the value of R$_{He}$ to be 109 721.636 cm^{-1}. This value should be accurate because it was calculated by both

determining the reduced mass of He^+ and finding the mass ratio of H to He^+ and multiplying the determined value by the constant determined for H. A literature value for R_{He} was unable to be found from an accurate source. Therefore, the estimated R_{He} value was used for data comparison.

When the 95% confidence interval is applied, each calculation for R_H and R_{He} were determined to be significant. All values, when their respective confidence interval was applied, overlapped with the accepted literature values, or the estimated calculated value. Although the confidence intervals overlap, the range of the confidence intervals were quite large, particularly for He, indicating much error in data acquisition or calculation. This is evident in the He II line spectrum from the acquired data, Figure 4, which showed transitions all over the range of the spectrum with varying intensities. This made it difficult to differentiate the important peaks for He^+ from the peaks from He, which contribute most of the contents of the lamp, and therefore contribute most of the peak values with high intensities in the spectrum. Another source of error is that the high-resolution scans were not taken in the correct estimated areas. Since this was the case, the measurements had to be taken on the less accurate low-resolution survey scans, and this may have contributed to some shifting of the peak centers. This is easily remedied by predicting peak locations correctly and taking high resolution scans in the correct locations. The analysis of the H spectrum did not have many outstanding errors, but it is not free of them. Better data can always be taken.

A way to improve results would be to take data from a wider range of wavelengths or use a more sensitive or powerful instrument to collect data, so different transitions can be observed, and the important peaks made more evident, especially towards the blue end of the energy spectrum where the intensities of the peaks are very similar to the excess noise detected.

The values for energy level locations of the He II spectrum were taken from the National Institute of Standards and Technology (NIST), a standard database that reports the most accurate values, as opposed to other relevant literature. From this data, the transition energies may be calculated for any relevant transition. In order to minimize the effect of spin-orbit coupling to the system, the ns transitions were chosen for comparison. Table 7 below tabulates the transition values from NIST energy level data in comparison to the measured peak values from the He II spectrum [8]. In extension, the value of R_{He} may be calculated using these known transition values from NIST in an attempt to determine a comparison value for the region measured. When all the values were calculated and averaged, the value of R_{He} for this range of data was determined to be 109 727.2824 cm^{-1}, which is still within the range of the values determined by measurement, with the 95% confidence interval applied.

Table 7. Tabulated transition values of NIST data compared to acquired data, with respective transition and percent error values.

Respective Transition / n_1 to n_2	NIST Transition Value / cm^{-1}	Measured Transition Value / cm^{-1}	Percent Error / %
4 to 6	15239.97191	15231	0.058871
4 to 7	18474.54432	18309	0.896067
4 to 8	20573.8968	20302	1.321562
4 to 9	22013.20077	22355	1.552701
4 to 10	23042.72339	22918	0.54127
4 to 11	23804.45183	23958	0.64504
4 to 12	24383.80758	24247	0.561059
4 to 13	24834.68179	24819	0.063145
4 to 14	25192.43612	25192	0.001731
4 to 15	25481.05367	25445	0.141492
4 to 16	25717.26571	25707	0.039918
4 to 17	25913.03226	25848	0.250964
4 to 18	26077.08638	26160	0.317956

Observing trends in the error data, it can be concluded the data acquired is accurate, with several values only differentiated by fractions of an inverse centimeter on the low end, and the highest percent error between the values being only 1.55%. With more sensitive instrumentation or analysis, the centers of the measured peaks may be calculated out to a more accurate decimal place, allowing for more precise acquisition of data and accurate analysis of the calculation of the Rydberg constant for He. Also, once again, by taking high resolution scans in the correct areas of the analyzed spectrum, more accurate data may also be acquired.

The differentiation between the values of R_{He} calculated from the NIST data, with a value of 109 727.2824 cm^{-1}, and the estimated calculated mass, with a value of 109 721.636 cm^{-1}, stems from the relativistic relationship between mass and energy. The variable component of the equation used to calculate R_X, Equation 2, is the reduced mass. Since the electron is invariably moving throughout the system of the He$^+$ atom, the relativistic mass of the electron gives a better estimation to the reduced mass of the atom, as opposed to the known rest mass of the electron m_0 (9.10939 x 10^{-31} kg). This relativistic mass is determined by the equation:

$$(8) \qquad m_{rel} = \frac{m_0}{\sqrt{1-\frac{v^2}{c^2}}}$$

where v is the speed of the electron, and m_{rel} is the relative mass [9]. So long as the electron is moving slower than the speed of light, its relativistic mass will be greater than that of its rest mass. When substituted into Equation 3, the reduced mass of

He$^+$ will be greater than that of the reduced mass using the rest mass of an electron. Therefore, once substituted into Equation 2 to solve for the Rydberg constant, it will yield a larger value.

References

[1] Kolasinski, K.W. *Physical chemistry: How chemistry works,* 1st ed.; Wiley: Chichester, **2017**.

[2] National Institute of Standards and Technology, https://physics.nist.gov/cgi-bin/cuu/Value?ryd|search_for=rydberg (accessed 7 April 2020).

[3] Pohl, R.; Antognini, A.; Nez, F.; Amaro, F. D.; Biraben, F.; Cardoso, J. M. R.; Covita, D. S.; Dax, A.; Dhawan, S.; Fernandes, L. M. P.; Giesen, A.; Graf, T.; Hänsch, T. W.; Indelicato, P.; Julien, L.; Kao, C. Y.; Knowles, P.; Le Bigot, E. O.; Liu, Y. W.; Lopes, J. A. M.; Ludhova, L.; Monteiro, C. M. B.; Mulhauser, F.; Nebel, T.; Rabinowitz, P.; dos Santos, J. M. F.; Schaller, L. A.; Schuhmann, K.; Schwob, C.; Taqqu, D.; Veloso, J. F. C. A.; Kottmann, F., The size of the proton. *Nature* (London) **2010,** *466*, 213-216.

[4] Bernauer, J. C.; Achenbach, P.; Ayerbe Gayoso, C.; Böhm, R.; Bosnar, D.; Debenjak, L.; Distler, M.O.; Doria, L.; Esser, A.; Fonvieille, H.; Friedrich, J.M.; Friedrich, J.; Gómez Rodríguez de la Paz, M.; Makek, M.; Merkel, H.; Middleton, D.G.; Müller, U.; Nungesser, L.; Pochodzalla, J.; Potokar, M.; Sánchez Majos, S.; Schlimme, B.S.; Širca, S.; Walcher, T.; Weinriefer, M., High-precision determination of the electric and magnetic form factors of the proton. *Phys. Rev. Lett.* **2010,** *105*, 242001.

[5] Mohr, P.J.; Newell, D.B.; Taylor, B.N., CODATA recommended values of the fundamental physical constants. *Rev. Mod. Phys.* **2016,** *88*, 035009.

[6] Beyer, A.; Maisenbacher, L.; Matveev, A.; Pohl, R.; Khabarova, K.; Grinin, A.; Lamour, T.; Yost, D. C.; Hänsch, T. W.; Kolachevsky, N.; Udem, T., The Rydberg constant and proton size from atomic hydrogen, *Science.* **2017**, *358*, 79-85.

[7] Kolasinski, K. W., Barth, R. *Experimental Physical Chemistry I.* Department of Chemistry West Chester University: West Chester, 2020.

[8] Mohr, P. J.; Taylor, B. N.; Newell, D. B., CODATA recommended values of the fundamental physical constants: 2006, *Rev. Mod. Phys.* **2008,** *80*, 633-730.

[9] Murray, R. L.; Holbert, K. E. *Nuclear energy: An introduction to the concepts, systems, and applications of nuclear processes,* 8th ed; Elsevier, **2020**.